

A Control Strategy for Stable Passive Running

M. Ahmadi and M. Buehler

Centre for Intelligent Machines, Department of Mechanical Engineering
McGill University
Montreal, Quebec, H3A 2A7

Abstract

We present a control strategy for a simplified model of a one legged running robot which features compliant elements in series with hip and leg actuators. Proper spring selection and initial conditions result in "passive dynamic" operation close to the desired motion, without any actuation. However, this motion is not stable. The proposed controller is based on online calculations of the desired passive dynamic motion and stabilises any fixed robot speed. It also tracks large changes in desired robot velocity and remains largely passive for a wide range of velocities, despite a fixed set of springs, masses and inertias. To this end, the desired motion is expressed as a function of a normalized "locomotion time" parameter. Comparisons of simulated runs with direct hip actuation show dramatic energy savings of 95% at 3m/s. Such energy savings are critical for the power autonomy of electrically actuated legged robots.

1 Introduction

Research in dynamically stable legged locomotion aims at understanding the design, dynamics and control of legged machines with the goal of maximizing dexterity, mobility, speed and efficiency. Progress in this direction has been difficult due to the high dimensionality, the intermittent and under-actuated nature of locomotion, analytically intractable models, and in practice the multitude of constraints on actuator systems. Despite these difficulties the robotics community has been able to produce over the past 15 years several working dynamically stable monopods [12, 4], bipeds [10, 1, 3, 5, 16] and quadrupeds [11, 2]. The largest contribution to date is the pioneering work of Raibert and coworkers [14] who have built one-, two- and four-legged hydraulically actuated robots, based on prismatic compliant legs. With their elegant mechanical designs, apparently complex dynamical behaviour can be achieved by relatively simple control algorithms.

In order to exploit the newly gained mobility and speed it is important to achieve autonomous operations and eliminate the highly constraining power cord on existing systems. Power autonomy in dynamic legged robots is an additional constraint on an already challenging design and control problem, and has only recently received attention in the research community. McGeer [8] has built completely un-actuated gravity powered legged mechanisms capable of walking down

inclines. Such unforced motion of a mechanical system is called its "passive dynamics." From the very beginning have Raibert's robots [14] exploited this principle for the vertical motion which is largely produced by a spring-mass system formed from body and compliant leg. Others [12, 4] and more recently [6] have succeeded in building electrically actuated robots using a similar design for the vertical dynamics.

Only recently has the robotics community investigated compliant elements to facilitate leg swinging motion. McGeer [7] studied a passive dynamic running biped without torso where two legs were connected via a spring. Based on linearized numerical analysis, he proposed strategies to achieve stable steady speed running. Raibert investigated a hip compliance for his one legged robot and showed that proper selection of the initial conditions allows, in principle, operation at any speed [15]. Subsequent experiments with a suitably modified biped confirmed this approach.

In this work we offer a control algorithm that stabilizes a simplified model of Raibert's one legged robot with a compliant hip. The control problem for the compliant hip (fore-aft swinging) is much more difficult than that for the compliant leg (vertical oscillation) control for three reasons. First, the leg spring is "reset" by a hard-stop to a nominal length at each lift-off. This is not the case for the hip spring. Second, in addition to controlling forward speed during flight via touchdown foot placement and body pitch during stance, the hip motion has to remain close to its passive motion if energy minimization is to be realized. Third, it is a coupled oscillation which has to remain closely synchronized with the vertical motion to achieve stable locomotion.

2 Problem Statement

The most elementary prototype model for the study of dynamically stable locomotion is shown in Fig. 1 together with one complete locomotion cycle. This model is based on Raibert's earliest experimental robot [13], and later similar robots [12, 4] built to study the control and energetics of electrically actuated variants. As in [15], we make the simplifying assumptions of negligible frictional losses, zero toe mass, zero spring preload, and a total centre of mass located at the hip joint.

The central idea underlying the use of passive dynamic motion in the hip is illustrated in Fig. 2. If we

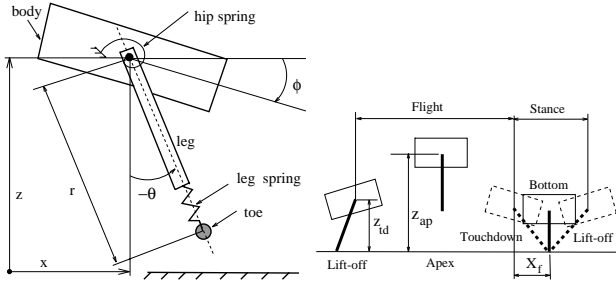


Figure 1: *Left: Model of the simplified passive monopod. Actuators for control will be in series with each of the springs. Right: Locomotion phases during one cycle*

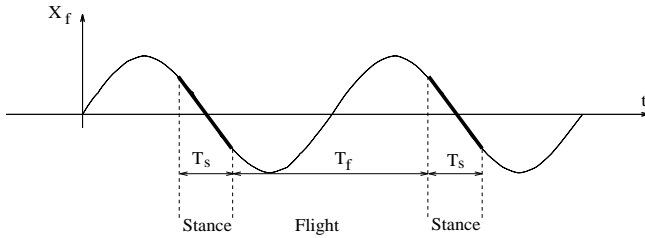


Figure 2: *Hip oscillations with linear approximations of stance phase.*

denote by x_f the horizontal position of the toe with respect to the hip in Fig. 2, a completely unforced, frictionless oscillation of the leg inertia – hipspring – bodyinertia system produces a sinusoidal response. It can now be seen that, with proper initial conditions and coordination with the vertical motion, one can achieve that stance phase occurs during the period of approximately constant slope, equivalent to the robot forward speed. Thus the unforced response can provide for the correct gross hip motion during locomotion.

Two questions must be answered before this idea can be used in practice. Given the robot’s design parameters and a desired forward velocity, how to select the passive hip motion and the robot’s initial conditions? The answer to this question was given by Raibert and Thompson in [15]. Sec. 3 reviews and further elaborates their work in order to prepare for the answer to the second question, the central contribution of this paper, addressed in Sec. 4: How can a legged robot be actively stabilized for a fixed as well as varying velocity while exploiting the passive hip swinging? The answer to this question permits dramatic energy savings which should aid in the development of power autonomous dynamic legged robots.

3 Passive Running

In this section, we derive the initial conditions that result in passive dynamic running, given the robot’s design parameters and the desired forward speed. Since the variables in this section correspond to the passive dynamic case they bear the superscript “*”.

g	gravitational acceleration	9.81
J_b	body inertia	2.5
J_l	leg inertia	0.25
J_{eff}	effective inertial (1)	0.227
k_h	hip spring stiffness	37.8
k_l	leg spring stiffness	18120
m_b	body mass	10
m_l	leg mass	1
m	total mass ($m_b + m_l$)	11
r	leg length (Fig. 1)	
r_0	maximum leg length	0.7
T_f	flight period	
T_s	stance period (4),(5)	
T_{step}	step period (1)	0.5
x	hip horizontal position (Fig. 1)	
x_f	foot position w.r.t hip (Fig. 1)	
z	hip vertical position (Fig. 1)	
θ	leg angle w.r.t. vertical (Fig. 1)	
ρ	duty factor (6)	
ϕ	body pitch angle (Fig. 1)	
ω_h	hip oscillation frequency (1)	
ω_l	vertical natural frequency (3)	

Table 1: *Nomenclature and numerical settings.*

3.1 Hip Oscillation

The natural frequency, period of oscillations and effective inertia of the body-leg counter oscillation (Fig. 1) can be derived from robot’s equations of motion as

$$\omega_h = \sqrt{\frac{k_h}{J_{eff}}}, \quad T_{step} = \frac{2\pi}{\omega_h}, \quad J_{eff} = \frac{J_b J_l}{J_b + J_l}. \quad (1)$$

A symmetric counter-oscillation between leg and body requires the hip spring to be at rest at the initial configuration, $\theta_0^* = \phi_0^* = 0$. Then given initial leg speed, $\dot{\theta}_0^*$, the following relations will be true for the leg and body amplitudes of speed.

$$\dot{\theta}_0^* = \dot{\theta}^*, \quad \dot{\phi}_0^* = \dot{\phi}^* = -\frac{J_l}{J_b} \dot{\theta}^*. \quad (2)$$

3.2 Vertical Oscillations

Flight: In this phase the purely ballistic robot motion is described by $z(t) = z_{lo} + \dot{z}_{lo}t - gt^2/2$ which is a function of the liftoff height, z_{lo} , and the lift-off velocity \dot{z}_{lo} .

Stance: Without pre-load in the spring, the centre of mass will follow a sinusoidal motion with a natural frequency

$$\omega_l = \sqrt{\frac{k_l}{m}} \quad (3)$$

resulting in the stance time

$$T_s = \frac{2}{\omega_l} (\pi - \text{Arctan}(-\dot{z}_{lo}\omega_l/g)). \quad (4)$$

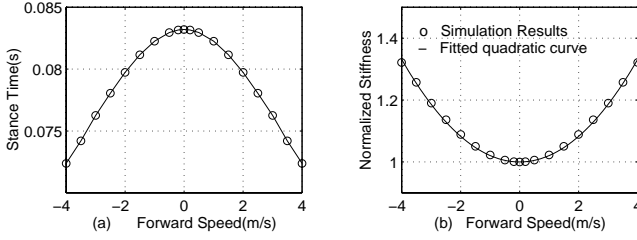


Figure 3: (a) Measured stance times (b) Normalized leg stiffness as a function of lift-off speed at steady state.

Assumes gravitational forces are small compared to the leg spring forces, this expression can be simplified to

$$T_s \approx \frac{\pi}{\omega_l}, \quad (5)$$

which is half of the period of vertical oscillation. This expression for the stance time was used in [15].

3.3 Leg Spring Stiffening Effect

Accurate knowledge of stance time is important since it is the basis for both the purely passive motion, via the calculation of the initial conditions, and, more critically, for the stabilizing control algorithm proposed in Sec. 4. However, being derived for vertical operation, neither (5) nor (4) are accurate enough for non-zero forward speeds. On the other hand, a closed form solution for the stance time from the planar dynamics, even in our simplified case, is not available. Therefore, we obtain the relation between the stance time and forward velocity via simulations at a multitude of speeds (steady states) and use a linear interpolation between the data points instead of the above approximate analytical relationships (4) or (5). The resulting relationship is captured in Fig. 3 (a) which shows a considerable drop in the stance time as speed increases.

For each running speed, the speed dependent vertical stance oscillation frequency $\omega_l(x)$ can be found via (4) or (5) starting from the corresponding computed stance time. Based on the computed ω_l an equivalent vertical leg stiffness k_v can be defined via (3), $k_v = m\omega_l^2 = m(\pi/T_s)^2$. The computed “normalized stiffness” $k_{norm} = k_v/k_l$ can be approximated accurately with the second order polynomial, $k_{norm} = 0.02\bar{x}^2 + 1$ as shown in Fig. 3 (b). This result is consistent with McMahon [9] who found similar increases in equivalent vertical stiffness in a human runner in terms of the forward speed.

3.4 Selection of Initial Conditions

For purely vertical hopping, the robot design parameters m, J_b, J_l, k_h, k_l determine the hip and leg oscillation frequencies, as well as the duty factor as follows,

$$\omega_h = \sqrt{\frac{k_h}{J_{eff}}}, \quad \omega_l = \pi\sqrt{\frac{m}{k_l}}, \quad \rho = \frac{T_s}{T_{step}} = \frac{1}{2}\sqrt{\frac{k_h m}{k_l J_{eff}}}. \quad (6)$$

Due to the planar hopper dynamics, these relationships are not correct at non-zero forward speeds. The hip oscillation frequency and the step time is still determined from the robot’s design parameters via the first equation above. Then, however, the velocity dependent stance time during steady state passive run is computed as

$$T_s = \frac{m\pi}{\sqrt{k_l(0.02\bar{x}^2 + 1)}} \quad (7)$$

from the relationship developed in the previous section. Now the duty factor ρ is determined via $\rho = T_s/T_{step}$.

The initial conditions are selected to accommodate a desired forward speed \dot{x}_d . Some of the initial conditions, namely $\phi_0^* = 0, \theta_0^* = 0, \dot{z}_0 = 0, x_0 = 0$ are known because we have selected a symmetric oscillatory hip motion.

Initial Angular Leg Speed: In [15] the desired speed is assumed to be equivalent to the maximum speed at the mid stance $\dot{\theta}_0^* = \dot{x}/r_0$. We observed greatly improved behaviour when relying on *average speed*, which also depends on the stance time. This has two reasons. First, the average speed is a better approximation of the sinusoidal curve during stance time. In addition, the dependency on T_s takes some coupling effects between vertical and horizontal dynamics as well as the spring stiffening effect into account. The measured average speed of stance is computed as

$$\bar{x} = \frac{x_{f,td} - x_{f,lo}}{T_{s,m}} \approx \frac{2}{T_{s,m}}x_{f,td} \quad (8)$$

where $T_{s,m}$ is the measured stance time and the approximation assumes symmetric operation at steady state, $x_{f,lo} = -x_{f,td}$. The foot position with respect to the hip is described by $x_f = -r_0 \sin[\theta^*(t)] = -r_0 \sin[\hat{\theta}^* \sin \omega_h t]$, therefore

$$\bar{x} = -\frac{2r_0}{T_s} \sin\left[\frac{\hat{\theta}_0^*}{\omega_h} \sin((1-\rho)\pi)\right].$$

Now this equation can be solved for $\hat{\theta}_0^*$

$$\hat{\theta}_0^* = -\frac{\omega_h \arcsin(T_s \bar{x}/2r_0)}{\sin((1-\rho)\pi)}. \quad (9)$$

Initial Body Pitch Speed: At steady state, a zero total angular momentum is assumed during flight. Based on the derivation of $\hat{\theta}_0^*$ in (9), and from (2) we can now calculate the initial body pitch speed as

$$\dot{\phi}_0^* = -\frac{J_l}{J_b}\hat{\theta}_0^*. \quad (10)$$

Initial Hip Vertical Position: At the initial condition the robot is located at “apex” z_{ap} which can be evaluated by adding the height at touchdown z_{td} and the change of height during the flight phase. Knowing that $t_{td} = T_f/2$ and $\theta_{td}^* = \hat{\theta}^* \sin((1 - \rho)\pi)$ (see Fig. 1) the initial height can be expressed as

$$z_0^* = z_{ap} = \frac{g}{8}(1 - \rho)^2 T_{step}^2 + r_0 \cos \left[\hat{\theta}^* \sin((1 - \rho)\pi) \right]. \quad (11)$$

3.5 Results

Using the nominal parameters given in Table 1 we start the robot with the appropriate initial conditions to obtain completely passive runs. Fig. 4 shows simulation runs for forward speeds of 1, 2 and 3 m/s and confirms the ability of the robot to run for a few cycles just by synchronizing the vertical and hip oscillations through proper selection of initial conditions in spite of all modelling approximations. At higher speeds small errors lead to faster failure. It can be seen from the data that only the amplitude of the leg-body oscillation needs to be modified to accommodate a desired forward speed, based on a fixed set of robot parameters. Thus the hip “natural oscillation” would be a good basis to define a desired trajectory for control as well.

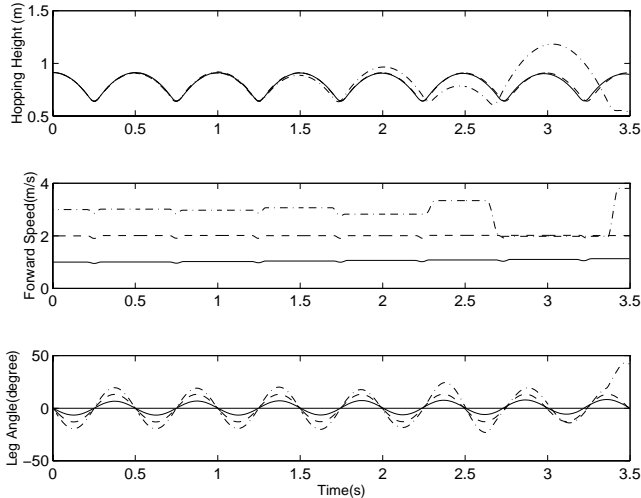


Figure 4: *Uncontrolled Passive Running.*

4 Controlled Passive Running

The two control inputs are the leg and hip actuators displacements. While the robot with four degrees of freedom, x, z, ϕ, θ , is not controllable in the classical sense, it is possible to stabilize a coupled oscillations of those states by proper periodic forcing. The task of the controller is threefold. First, it computes and tracks the passive trajectory based on the current speed. Second, it adds a feedback term to modulate the passive trajectory to stabilize a desired forward speed. Third, it modulates the trajectory to accommodate variable speed tracking while still remaining

close to the passive trajectory to minimize energy consumption.

4.1 Locomotion Time

Successful locomotion must be based on robust coupling between different degrees of freedoms. This is accomplished via a scalar variable termed “locomotion time”. In our runner, the vertical dynamics determined by gravity during flight and the spring forces during stance, act as the “pacemaker,” to which the leg swing must synchronize. To achieve this synchronization, time is not a suitable parameter because flight or stance times are subject to variations during a run. Thus it is desirable to develop a new variable, termed locomotion time, which characterizes the dominating dynamics, in our case the vertical motion, independent of the operating conditions (e.g. the hopping height). A locomotion time satisfies two conditions:

Condition LT 1: η is a scalar valued function $\eta : \mathcal{Z} \mapsto \mathcal{E}$ which maps one flight phase, expressed in vertical body velocities, $\mathcal{Z} = (z_{lo}, -z_{lo})$ onto the fixed interval $\mathcal{E} = (-1, +1)$ between lift-off ($\eta(z_{lo}) = -1$) and touchdown ($\eta(\dot{z}_{td}) = +1$). In addition, $\eta(\dot{z} = 0) = 0$ at apex.

Condition LT 2: η is an affine function of time.

With these conditions satisfied, η becomes a “time-like” parameter suitable for motion planning with synchronization. One such measure during flight time is

$$\eta_1 = \frac{-\dot{z}}{\dot{z}_{lo}}. \quad (12)$$

It is easy to verify that η_1 satisfies condition LT 1, and compliance with condition LT 2 is also assured since

$$\eta_1 = -\frac{1}{\dot{z}_{lo}}(\dot{z}_{lo} - g(t + \frac{T_f}{2})) = \frac{g}{\dot{z}_{lo}}(t + \frac{T_f}{2}) - 1 = \frac{2}{T_f}t.$$

However, in practice, a measure depending on a single, possibly noisy velocity reading \dot{z}_{lo} , is not desirable. Therefore we use a variant of (12),

$$\eta_f = \frac{-\dot{z}(t)}{\sqrt{E_{vert}(t)}} \quad (13)$$

where the single lift-off velocity measurement \dot{z}_{lo} is replaced with the square root of the continuous measurement of the vertical total energy $E_{vert} = 2g(z - z_{lo}) + \dot{z}^2$. This new measure is equivalent to η_1 since at lift-off, the denominator is $\sqrt{E_{vert,lo}} = \dot{z}_{lo}$ and, assuming no energy losses during flight, $\dot{E}_{vert} = 0$. During stance, we use the locomotion time

$$\eta_s = \frac{2}{T_s}t \quad (14)$$

which maps the stance time interval $(-\frac{T_s}{2}, +\frac{T_s}{2})$ onto the interval $(-1, +1)$. In summary, we have now at our disposal a scalar quantity which maps both the stance and flight phases onto a fixed scalar interval and which can now form the basis for control.

4.2 Control during Flight Phase

A simple foot placement algorithm [14] is used to find the foot position, touchdown angle and the desired amplitude of leg oscillation in flight phase.

First, given the current forward speed, we obtain the “passive” leg touchdown angle, θ_{td}^* , required for passive dynamic operation at that speed from Fig. 5. The corresponding passive foot touchdown angle with respect to the hip is $x_{f,td}^* = -r_0 \sin \theta_{td}^*$. Forward speed can now be controlled towards the desired one by simply adding a proportional and a derivative error term, to obtain the desired foot touchdown position with respect to the hip,

$$x_{f,td,d} = x_{f,td}^* + \kappa \dot{x} (\dot{x} - \dot{x}_d). \quad (15)$$

A translation of the control law (15) in the desired leg touchdown angle is

$$\theta_{d,td} = -\sin^{-1} \left[-\sin(\theta_{td}^*) + \frac{k \dot{x}}{r_0} (\dot{x} - \dot{x}_d) \right]. \quad (16)$$

The resulting desired amplitude of oscillation $\hat{\theta}_d$, is

$$\hat{\theta}_d = \frac{\theta_{d,td}}{\sin(\pi(1-\rho))}. \quad (17)$$

The desired leg angle trajectory can be expressed in the time domain as $\theta_d(t) = \hat{\theta}_d \sin(w_h t)$, where $\hat{\theta}_d$ is the desired amplitude of oscillation. Finally, we can express the leg angle trajectory in η ,

$$\theta_d(\eta) = \hat{\theta}_d \sin(\pi(1-\rho)\eta). \quad (18)$$

Fig. 5 shows how the desired path of the leg motion is generated where each block contains the corresponding equation number.

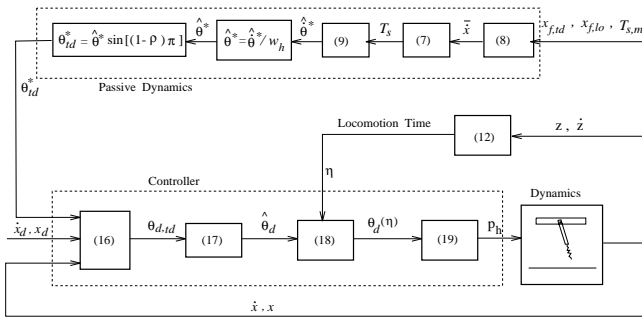


Figure 5: *Flight leg swing controller.*

Writing the equation of motion only for the leg angle as, $J_l \ddot{\theta} = k_h (p_h - \theta + \phi)$

this variable can now be tracked by recourse to a standard model based inverse dynamic controller of the form

$$p_h = \frac{J_l}{k_h} (\ddot{\theta}_d + k_v \dot{e}_\theta + k_p e_\theta) + \theta - \phi \quad (19)$$

resulting in the assignable error dynamics $\ddot{e}_\theta + k_v \dot{e}_\theta + k_p e_\theta = 0$, $e_\theta = \theta_d - \theta$. When the steady state error is zero, the actuator displacement p_h will also be zero.

4.3 Control during Stance Phase

During stance, the hip actuator p_h controls the body’s pitch angle ϕ . At the same time, the leg actuator controls the hopping height by introducing a displacement at bottom, p_l .

Pitch angle control: The controller uses again inverse dynamics to track the desired pitch trajectory $\phi_d = \hat{\theta}_d \sin(w_h t)$. The amplitude of the body oscillation $\hat{\phi}_0$ is proportional to the leg angle amplitude, $\hat{\phi}_d = -J_b/J_l \hat{\theta}_d$. Based on the hopper’s body equation of motion during the stance phase $-J_b \ddot{\phi} = -k_h (\theta - \phi + p_h)$, the controller takes the form

$$p_h = -\frac{J_b}{k_h} (\ddot{\phi}_d + k_v \dot{e}_\phi + k_p e_\phi) + \theta - \phi \quad (20)$$

where $e_\phi = \phi_d - \phi$. The desired pitch angle at touchdown ($\eta_s = 1$) is $\phi_{d,td}$, and the same magnitude but negative angle is expected at lift-off ($\eta_s = -1$). Thus the desired path in terms of locomotion variable η_s domain is found by the relation between η_s and t in a similar fashion as above, by changing the time interval from $T_f/2$ to $T_s/2$ and considering that $\phi_{d,td}$ is negative,

$$\phi_d = -\hat{\phi}_d \sin(w_h t) = -\hat{\phi}_d \sin(\pi \rho \eta_s). \quad (21)$$

Hopping height control: The hopping height is controlled by a proportional controller which is active intermittently during each decompression phase, $p_l = k_z (z_{ap} - z_{max})$, where z_{ap} is the desired body apex height obtained from (11) and z_{max} is the last hopping height.

4.4 Results

The effectiveness of our control strategy is shown in both steady state and transient operation. First, during steady state, Fig. 6 demonstrates that the robot leg (during flight) and pitch (during stance) angle trajectories (solid traces) are very close to the desired passive dynamic trajectories (dashed traces). This confirms that the desired passive trajectories are computed correctly, and the controller accomplishes stable and accurate tracking. At the same time, the actuator effort remains within $\pm 0.2 \text{ deg}$.

Fig. 7 shows simulation runs with ramp changes in commanded speed to demonstrate robust tracking performance of the controller, even though it was designed based on steady state operation. In fact, the same controller successfully tracks step inputs up to 2 m/s , provided that large actuator displacements can be accommodated.

To validate our main objective of reducing the energy requirements compared to direct actuation, we have run both compliant and direct actuation simulations with different desired speeds. By setting the spring stiffness to a high value, our approach can be directly applied to control a directly actuated hip as well. Fig. 8 shows the total hip energy consumed in three seconds and verifies that dramatic energy savings of approximately 95% are achievable when exploiting passive dynamics.

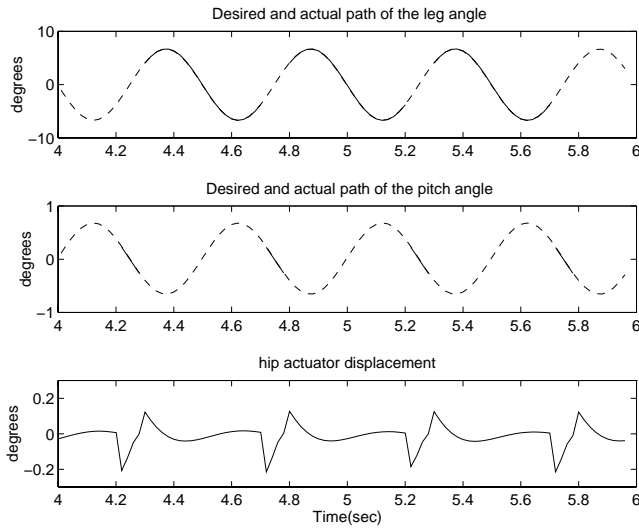


Figure 6: Simulation of controlled passive dynamic running at 1m/s steady state. Dashed: Desired trajectories for passive dynamic operation. Solid: Actual trajectories during controlled running.

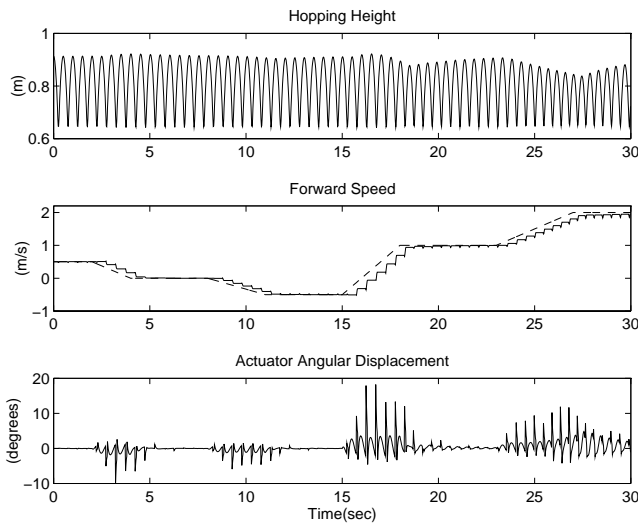


Figure 7: Hopping height, velocity variation and hip actuator displacement for velocity tracking.

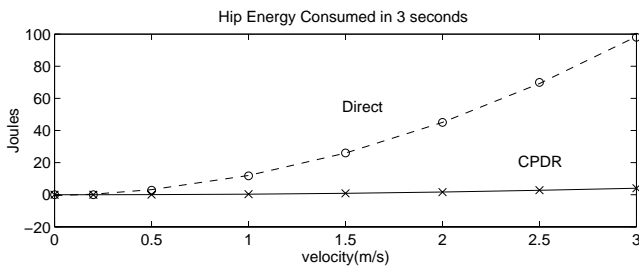


Figure 8: Energy consumption in the hip actuator.

References

- [1] A. Takanishi et al. The realization of dynamic walking robot WL-10RD. In *ICAR*, pages 459–466, 1985.
- [2] Y. Sakakibara et al. Foot trajectory for a quadruped walking machine. In *IEEE Int. Workshop on Intelligent Robots and Systems*, pages 315–322, 1990.
- [3] J. Furusho and M. Masubuchi. Control of a dynamical biped locomotion system for steady walking. *ASME J. Dynamics Systems, Measurement, and Control*, 108:111–118, Jun 1986.
- [4] P. Gregorio, M. Ahmadi, and M. Buehler. Experiments with an electrically actuated planar hopping robot. In T. Yoshikawa and F. Miyazaki, editors, *Experimental Robotics III*. Springer-Verlag, 1994.
- [5] S. Kajita, K. Tani, and A. Kobayashi. Dynamic walk control of a biped robot along the potential energy conserving orbit. In *IEEE Int. Workshop on Intelligent Robots and Systems*, pages 789–794, 1990.
- [6] A. Lebaudy, J. Prosser, and M. Kam. Control algorithms for a vertically-constrained one-legged hopping machine. In *Proc. IEEE Int. Conf. Decision and Control*, pages 2688–2693, 1993.
- [7] T. McGeer. Passive bipedal running. Technical Report IS-TR-89-02, Simon Fraser University, Centre for Systems Science, Apr 1989.
- [8] T. McGeer. Passive dynamic walking. *Int. J. Robotics Research*, 9(2), 1990.
- [9] T. A. McMahon and G. C. Cheng. The mechanics of running: how does stiffness couple with speed? *J. Biomechanics*, 23:65–78, 1990.
- [10] H. Miura and I. Shimoyama. Dynamic walk of a biped. *Int. J. Robotics Research*, 3, 1984.
- [11] H. Miura, I. Shimoyama, M. Mitsuishi, and H. Kimura. Dynamical walk of quadruped robot (Collie-1). In H. Hanafusa and H. Inoue, editors, *Int. Symp. Robotics Research*. MIT Press, Cambridge, 1985.
- [12] K. V. Papantoniou. Electromechanical design for an electrically powered, actively balanced one leg planar robot. In *Proc. IEEE/RSJ Conf. Intelligent Systems and Robots*, Osaka, Japan, 1991.
- [13] M. H. Raibert. Dynamic stability and resonance in a one-legged hopping machine. *4th Symp. Theory and Practice of Robots and Manipulators*, 1981.
- [14] M. H. Raibert. *Legged Robots That Balance*. MIT Press, Cambridge, MA, 1986.
- [15] M. H. Raibert and C. M. Thompson. Passive dynamic running. In V. Hayward and O. Khatib, editors, *Experimental Robotics I*, pages 74–83. Springer-Verlag, NY, 1989.
- [16] A. Sano and J. Furusho. Realization of natural dynamic walking using the angular momentum information. In *Proc. IEEE Int. Conf. Robotics and Automation*, pages 1476–1481, 1990.